Available online at www.sciencedirect.com
SCIENCE DIRECT®
International Journal of Heat and Mass Transfer 48 (2005) 5625–5638
International Journal of HEAT and MASS TRANSFER
www.elsevier.com/locate/ijhmt

Freezing-induced splashing during impact of molten metal droplets with high Weber numbers

Rajeev Dhiman, Sanjeev Chandra *

Centre for Advanced Coating Technologies, Department of Mechanical and Industrial Engineering, University of Toronto, 5 King's College Road, Toronto, Ont., Canada M5S 3G8

Received 4 August 2004; received in revised form 8 May 2005
Available online 4 October 2005

Abstract

The impact of molten tin droplets (0.6 mm diameter) on solid surfaces was observed for a range of impact velocities (10–30 m/s), substrate temperatures (25–200 °C) and substrate materials (stainless steel, aluminum and glass). The substrate was mounted on the rim of a rotating flywheel and the collision of single droplets with the moving substrate was photographed. Droplet impact Reynolds number ranged from 2.2×10^4 to 6.5×10^4 and Weber number from 8.0×10^2 to 7.2×10^3. On a hot surface there was no splashing and droplets spread to form disk-like splats with smooth edges. Solidification around the edges of droplets spreading on cold surfaces created a solid rim that obstructed flow and triggered splashing. An analytical model was developed to predict the transition temperature at which splashing disappeared by assuming that the thickness of the solid layer had to equal that of the splat in the time the droplet spread to its maximum extent in order to obstruct liquid flow. The model predicted the transition temperature for aluminum and stainless steel surfaces, assuming that thermal contact resistance between the droplet and substrate varied between 10^{-6} and 10^{-7} m^2 K/W. The model also predicted that tin droplets would not splash on glass surfaces maintained at or above room temperature, and this was confirmed by experiments.

Keywords: Splashing; Droplet impact; Thermal contact resistance; Molten metal spray

1. Introduction

Many industrial processes such as spray forming and thermal spray coating produce solid deposits by impingement and solidification of molten metal droplets onto a substrate. When a liquid droplet hits a solid surface it may, depending on impact conditions, splash and disintegrate into many small satellite droplets. Droplet splashing is undesirable in most applications since it not only results in wastage of material but also produces pores in the deposit and reduces its strength.

Because of its practical importance, many studies have been devoted to investigate molten metal droplet splashing. Several investigations have been done under thermal spray conditions [1–7] by observing solidified droplets after impact, commonly known as splats. Bianchi et al. [1] demonstrated that the shape of splats formed by spraying alumina or zirconia droplets from a plasma torch onto a stainless steel plate varied as surface temperature was increased. Droplets landing on a cold substrate (below 100 °C) splashed extensively after

* Corresponding author. Tel.: +1 416 978 5742; fax: +1 416 978 7753.
E-mail address: chandra@mie.utoronto.ca (S. Chandra).

0017-9310/$ - see front matter © 2005 Elsevier Ltd. All rights reserved.
doi:10.1016/j.ijheatmasstransfer.2005.05.044

Nomenclature

$A = \sqrt{\frac{8\pi\gamma_d}{3Pe\gamma_s}}$	
c	specific heat
D_0	droplet diameter before impact
D_{max}	droplet diameter at maximum spread
h	splat thickness
h^*	dimensionless splat thickness ($=h/D_0$)
H_f	latent heat of fusion
k	thermal conductivity
N	Number of droplets
N_f	Number of fingers
q_0	heat flux at the droplet–substrate interface
R_a	Average roughness of substrate surface
R_c	contact resistance at droplet–substrate interface
R_{th}	thermal resistance of solidified layer
s	thickness of droplet's solidified layer
s^*	dimensionless solid layer thickness ($=s/D_0$)
t	time
t^*	dimensionless time ($=tV_0/D_0$)
t_c	time to reach maximum spread
t_c^*	dimensionless time to reach maximum spread ($= t_cV_0/D_0$)
T_m	droplet melting temperature
T_s	substrate surface temperature
$T_{s,i}$	substrate initial temperature
T_t	transition temperature
V_0	droplet impact velocity

Greek symbols

α	thermal diffusivity
σ	droplet surface tension
ρ	density
θ_a	advancing contact angle
γ	$=k\rho c$
μ	droplet viscosity
ξ_{max}	maximum spread factor ($=D_{max}/D_0$)

Dimensionless numbers

Re	Reynolds number ($=\rho V_0D_0/\mu$)
We	Weber number ($= \rho V_0^2D_0/\sigma$)
Ste	Stefan number ($=c(T_m - T_{s,i})/H_f$)
Pe	Peclet number ($=V_0D_0/\alpha$)
Bi	Biot number ($=D_0/(R_ck_d)$)

Subscripts

d	droplet
s	substrate

impact and had very irregular contours while those deposited on a hot surface (above 150 °C) were disk-like, almost perfectly circular. Other researchers [2–7] also observed this change of splat shape and showed that the "transition temperature", above which disk splats were obtained, was a complex function of particle and substrate material properties [2,3], surface contamination [4,5] and surface oxidation [6]. Fukomoto and Huang [7] conjectured that freezing along the bottom of an impinging droplet causes splashing: liquid flowing on top of the solid layer jets off and splashes. Delaying solidification, either by raising surface temperature or increasing thermal contact resistance at the droplet–substrate interface, is expected to suppress splashing. If droplet velocity is high enough a droplet will splash, irrespective of surface conditions [8]. Wan et al. [9] investigated the importance of solidification on droplet spreading during thermal spraying. Their numerical results showed that a substrate with high thermal diffusivity, and maintained at a lower temperature during spraying, produces smaller splats.

Studies of thermal spray particle impact have depended on examination of solidified splats; the impact process itself has rarely been observed due to the difficulty of observing small particles (~10 μm diameter) impacting at high velocities (~100 m/s). Studies of molten metal droplet impact [10–12] have largely been confined to photographing impact of millimeter size droplets with low impact velocities (1–4 m/s). The impact Weber number of such droplets is much lower than those in typical industrial applications ($We \sim 10^2$ in experiments, compared to $We \sim 10^3$ in applications) and in such cases droplet solidification suppresses splashing [10]. Mehdizadeh et al. [13] built an apparatus in which molten tin droplets impinged on a steel plate mounted on the rim of a rotating flywheel, giving impact velocities of up to 40 m/s and $We \sim 10^3$. Photographs of splashing droplets were compared with predictions from computer simulations that showed that freezing around the edges of a spreading droplet obstructs liquid flow and causes splashing.

The objectives of this study were to: photograph impact of tin droplets on solid plates for a range of impact velocities (10–30 m/s), substrate temperature (25–200 °C) and substrate materials (stainless steel, aluminum and glass); record the final splat shape for all combinations of these parameters and observe conditions under which splashing occurred; and develop an analytical model to predict the transition temperature at which droplets no longer splashed. Droplet size (0.6 mm diameter) and substrate roughness ($R_a = 0.04$ μm for aluminum and 0.01 μm for stainless steel and glass) were kept constant.

Droplet Reynolds number ranged from 2.2×10^4 to 6.5×10^4 and Weber number from 8.0×10^2 to 7.2×10^3. This range ensured that the "splash parameter" defined as $We^{0.5}Re^{0.25}$ was always much greater than 57.7, which has previously been proposed as a criterion for splashing [14]. We used a one-dimensional heat conduction analysis to model solidification in a spreading drop and calculate the variation of transition temperature with droplet and substrate properties, impact velocity and thermal contact resistance between the substrate and droplet.

2. Experimental apparatus and method

A detailed description of the experimental apparatus (see Fig. 1) has been given by Mehdizadeh et al. [13], so it will be described only briefly here. It consisted of a molten metal droplet generator [15] that can produce uniform-sized tin droplets (0.6 mm diameter) on demand. In order to achieve high impact velocities, the substrate was mounted on the rim of a rotating flywheel. Replaceable coupons of three different materials—aluminum, stainless steel (type-302) and soda lime glass, with thicknesses 1.5, 0.5, 1.0 mm respectively—were used as substrates. Table 1 lists thermal properties of the three materials and of tin. The substrates could be heated and maintained at a desired temperature by means of cartridge heaters inserted into the plate on which the substrate was mounted. Substrate temperature was allowed to reach steady value while rotating before drops were deposited.

An optical sensor ascertained the position of the flywheel and activated a timing unit that synchronized

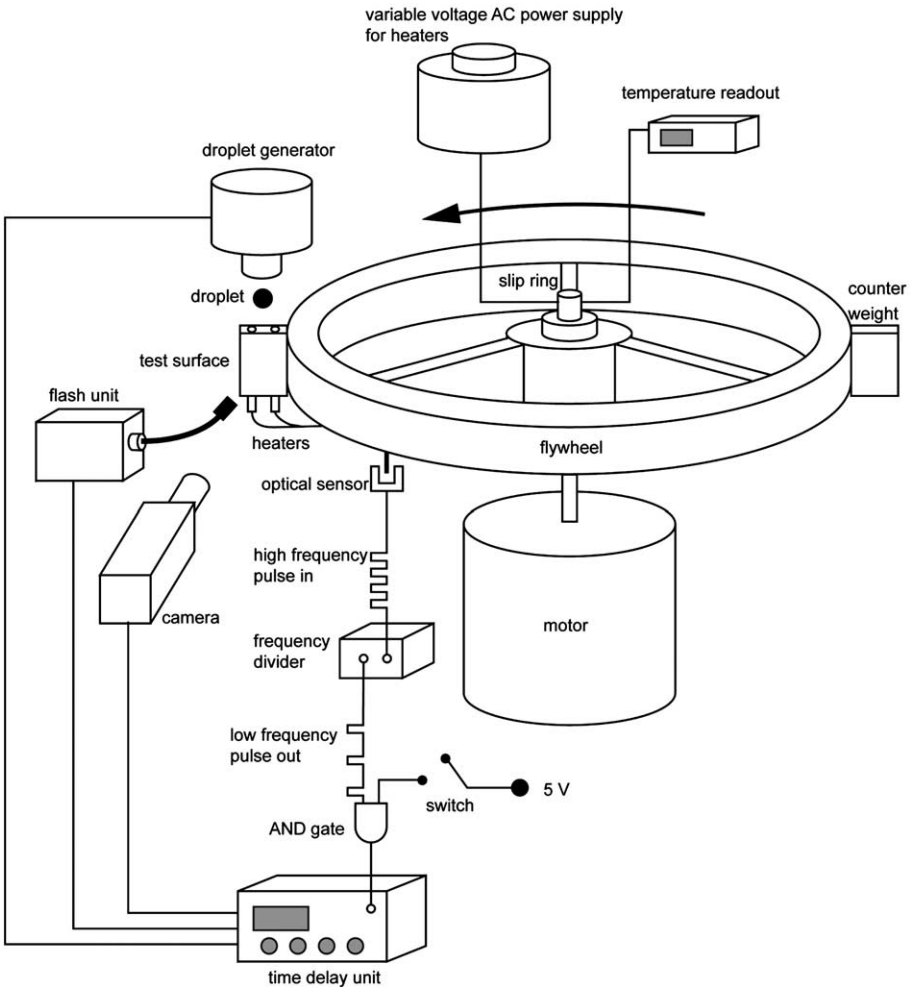

Fig. 1. Schematic diagram of the experimental apparatus.

Table 1
Thermophysical properties of materials used

Material	Density, ρ (kg m^{-3})	Thermal conductivity, k (W m^{-1} K^{-1})	Specific heat, c (J kg^{-1} K^{-1})	Surface tension, σ (N m^{-1})	Latent heat of fusion H_f (J kg^{-1})	Dynamic viscosity, μ (N s m^{-2})
Tin	6970	33.6	243	0.526	60,900	1.917×10^{-3}
Aluminum	2702	237	903	–	–	–
Stainless steel	8055	15.1	480	–	–	–
Glass	2800	0.7	750	–	–	–

droplet ejection with triggering of a high-resolution digital camera and flash so that a single photograph was taken when a falling droplet collided with the horizontally moving substrate. By varying the time delay before triggering the camera different stages of impact were photographed. Flywheel rotation was monitored by means of a digital motion controller and feedback system [16] that controlled angular velocity within ±0.5%. The vertical velocity of the droplet was less than 1 m/s, whereas the linear velocity of impact varied between 10 and 30 m/s: impact was therefore essentially normal. The entire droplet impact process took approximately 100–200 μs, depending on impact velocity. However, our ability to identify the instant of impact was accurate only within ±20 μs; sequences of droplet impact photographs therefore do not have exact times indicated on them. This was not a serious limitation as we did not make measurements of any time-dependent parameter.

An automatic grinding and polishing machine was used to prepare metal test surfaces. Each substrate was first ground with abrasive silicon carbide papers of successively finer grit size from 600 to 4000. After grinding the substrate was cleaned first with a water jet, then alcohol, and then buffed with diamond (3 and 9 μm size particles) and alumina (0.05 μm size particles) suspensions to get a mirror-polished finish. The average roughness of the substrate was measured to be 0.01 μm for stainless steel surfaces and 0.04 μm for aluminum surfaces.

3. Results and discussion

3.1. Transition temperature

Fig. 2 shows images of 0.6 mm diameter tin droplets impacting on a mirror-polished stainless steel substrate with 20 m/s velocity. Each column shows successive stages of droplet impact on a substrate at initial temperature ($T_{s,i}$) varying from 25 to 200 °C (indicated at the top of the column). The first picture in each sequence shows a droplet prior to impact, and the last shows the final splat shape.

Droplets hitting a cold substrate ($T_{s,i} = 25$–150 °C) splashed extensively, producing small satellite droplets and leaving a splat with irregular edges. The final splat surface was rough along the periphery, showing the region where it first solidified very rapidly; the centre was smoother, marking the area where surface tension forces had enough time to smoothen the surface before the onset of solidification. The extent of splashing decreased and eventually disappeared as substrate temperature was increased. No splashing was visible on a surface at 180 °C. Solidification did not start until fairly late during spreading; localized freezing at several spots acted to obstruct spreading of the splat and produced an irregular shaped splat even though there was no splashing. At $T_{s,i} = 200$ °C solidification was sufficiently delayed that droplets spread to form thin discs. Computer simulations [13] have shown that freezing around the droplet periphery during spreading on a substrate at low temperature obstructs liquid flow and triggers splashing. When substrate temperature is increased, freezing is slowed down and the droplet spreads in the form of a thin liquid sheet without any splashing. The transition temperature, though difficult to identify exactly, lies between $T_{s,i} = 150$ and 180 °C.

Photographs such as those shown in Fig. 2 were taken at three different impact velocities ($V_0 = 10$, 20 or 30 m/s); the final splat shapes for all combinations of impact velocity and surface temperature are displayed in Fig. 3. Reading across each row of Fig. 3 shows the effect of varying substrate temperature while scanning down each column shows the effect of increasing impact velocity.

In general, the final splat size increased as either the impact velocity or substrate temperature was increased. The larger initial momentum associated with high impact velocity forces a droplet to spread to a greater extent. Low substrate temperature promotes rapid freezing of an impacting droplet which restricts it from spreading freely; raising substrate temperature permits the droplet to remain liquid for a longer time and spread to a greater diameter. At the lowest surface temperature (25 °C) there was extensive splashing and a large portion of the initial droplet mass was lost. Therefore the effect of droplet impact velocity on final splat size was not very noticeable. At a surface temper-

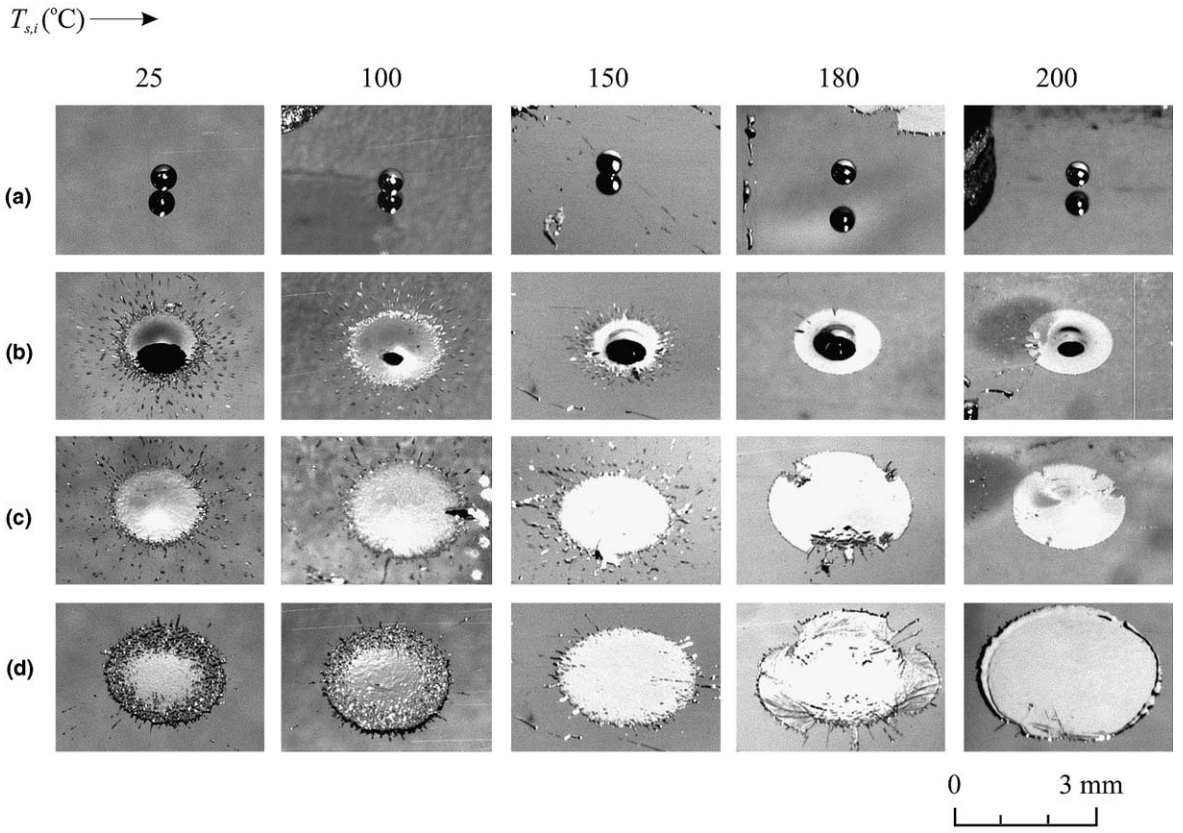

Fig. 2. Impact of molten tin drops with velocity 20 m/s on a stainless steel surface at temperature, $T_{s,i}$: (i) 25 °C, (ii) 100 °C, (iii) 150 °C, (iv) 180 °C and (v) 200 °C. The last picture in each column is the final solidified shape of the droplet. $Re = 43{,}636$, $We = 3180$.

ature of 100 °C splashing was somewhat reduced and the increase in splat diameter with impact velocity is apparent. At higher surface temperature (150 °C) solidification was so late that the spreading liquid had lost most of its momentum when it hit solid obstructions and the fingers of liquid formed due to instability did not detach but remained on the surface, radiating out from the splat. At $T_{s,i} = 180$ °C and 200 °C there was very little evidence of splashing. At the highest impact velocity (30 m/s) the edges of splats were irregular where the liquid hit solid patches on the surface. At low velocity ($V_0 = 10$ m/s) and high temperature ($T_{s,i} = 200$ °C) the splat remained liquid long enough that surface tension forces drew the molten metal back to the centre after impact. Traces of metal mark the maximum extent of spread. The solidified tin is not exactly at the centre because centrifugal forces due to substrate rotation pulled it to one side. As impact velocity increased the energy dissipated by viscous stresses in the droplet became larger [10] and droplet recoil became less evident. It is difficult to determine if impact velocity had any effect on transition temperature: in all cases it appeared to lie between 150 °C and 180 °C.

3.2. Predicting transition temperature

Numerical simulations [13] have shown that a molten tin droplet impacting on a colder substrate begins to freeze first around its periphery, where the substrate temperature is lowest. If the solid rim becomes thick enough it obstructs liquid flow and triggers an instability that leads to splashing. To derive an analytical expression to predict transition temperature, we assume that the thickness of the solidified layer (s) has to equal that of the splat (h) by the time (t_c) the droplet is at its maximum extension.

Heat transfer from the spreading splat to the substrate can reasonably be assumed to be one-dimensional: numerical simulations of molten metal droplet impact [11,13] have shown that temperature gradients in the substrate normal to the surface are several orders of magnitude greater than those in the radial direction. Radial heat conduction may therefore be neglected.

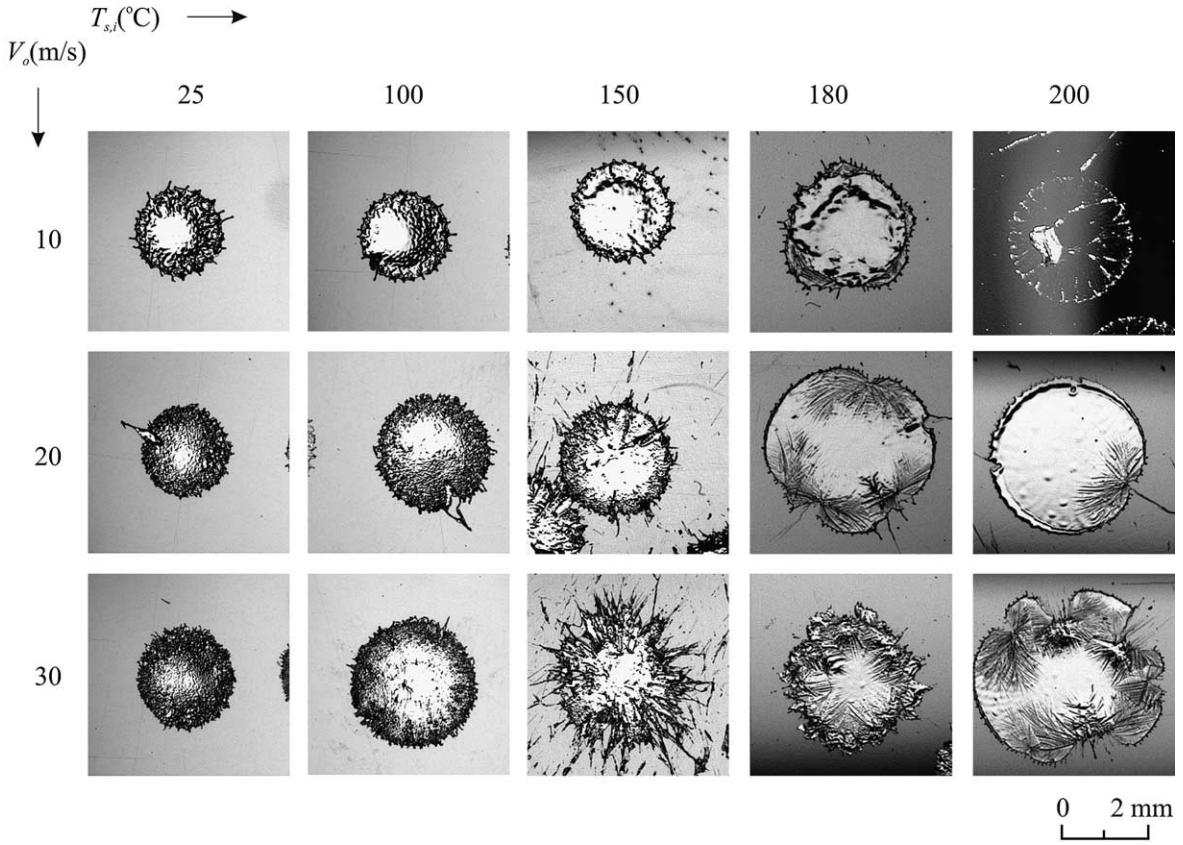

Fig. 3. Solidified splats of molten tin drops obtained on stainless steel surfaces with impact velocity, V_0 and substrate temperature, $T_{s,i}$.

An order of magnitude analysis of the Navier–Stokes equations has shown that centrifugal forces also have little impact on fluid flow during droplet spreading [17].

Poirier and Poirier [18] developed an analytical model for solidification of a molten metal in contact with a solid, semi-infinite substrate that accounts for thermal contact resistance at the droplet–substrate interface. The substrate is assumed to be isotropic with constant thermal properties. At time $t = 0$, the molten droplet at its melting point is suddenly brought into contact with the substrate whose initial surface temperature ($T_{s,i}$) is below the melting point of the droplet (T_m).

The contact resistance (R_c) at the melt–substrate interface is assumed to be constant so the surface temperature T_s is given by

$$T_s = T_m - q_0 R_c \tag{1}$$

where q_0 is the heat flux leaving the bottom surface of the splat. It is assumed that there is no temperature drop across the solidified layer. Calculations of the temperature drop across the solid layer shows that it increases from 0 to a maximum of 12 °C while the molten tin is at its melting point of 232 °C.

The thickness of the solid layer as a function of time (t) is given by [18]:

$$s = \frac{2}{\sqrt{\pi}} \frac{(T_m - T_{s,i})}{\rho_d H_{f,d}} \sqrt{\gamma_s t} \left\{ 1 - R_c \sqrt{\frac{\gamma_s}{\pi t}} \ln\left(1 + \frac{1}{R_c} \sqrt{\frac{\pi t}{\gamma_s}} \right) \right\} \tag{2}$$

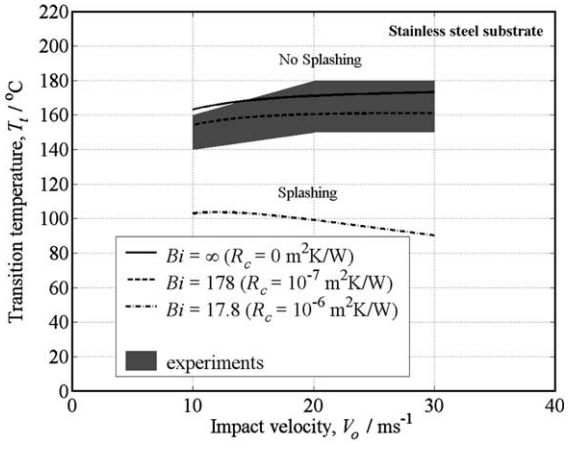

Fig. 4. Variation of transition temperature, T_t for stainless steel substrate with impact velocity, V_0 for different values of contact resistance, R_c at the droplet–substrate interface.

Eq. (2) can be written in non-dimensional form as

$$s^* = \frac{2}{\sqrt{\pi}} Ste \times \sqrt{\frac{\gamma_s t^*}{\gamma_d Pe}} \left\{ 1 - \frac{1}{Bi} \sqrt{\frac{\gamma_s Pe}{\gamma_d \pi t^*}} \ln \left[1 + Bi \sqrt{\frac{\gamma_d \pi t^*}{\gamma_s Pe}} \right] \right\} \quad (3)$$

Note that if $Bi \to \infty$ (or $R_c \to 0$), Eq. (3) reduces to the one obtained by Aziz and Chandra [10] for the case of zero contact resistance.

Splat thickness is estimated by assuming that the solidified splat is a thin cylindrical disc with a volume equal to that of the initially spherical droplet. The splat thickness (h) is [19]:

$$h = \frac{2D_0}{3\xi_{max}^2} \quad (4)$$

where ξ_{max} is the maximum splat diameter (D_{max}) non-dimensionalized by the initial droplet diameter (D_0) which can be calculated from the following analytical expression [10]:

$$\xi_{max} = \frac{D_{max}}{D_0} = \sqrt{\frac{We + 12}{\frac{3}{8} We s^* + 3(1 - \cos\theta_a) + 4\frac{We}{\sqrt{Re}}}} \quad (5)$$

Substituting ξ_{max} from Eq. (5) into Eq. (4) gives an expression for the dimensionless splat thickness:

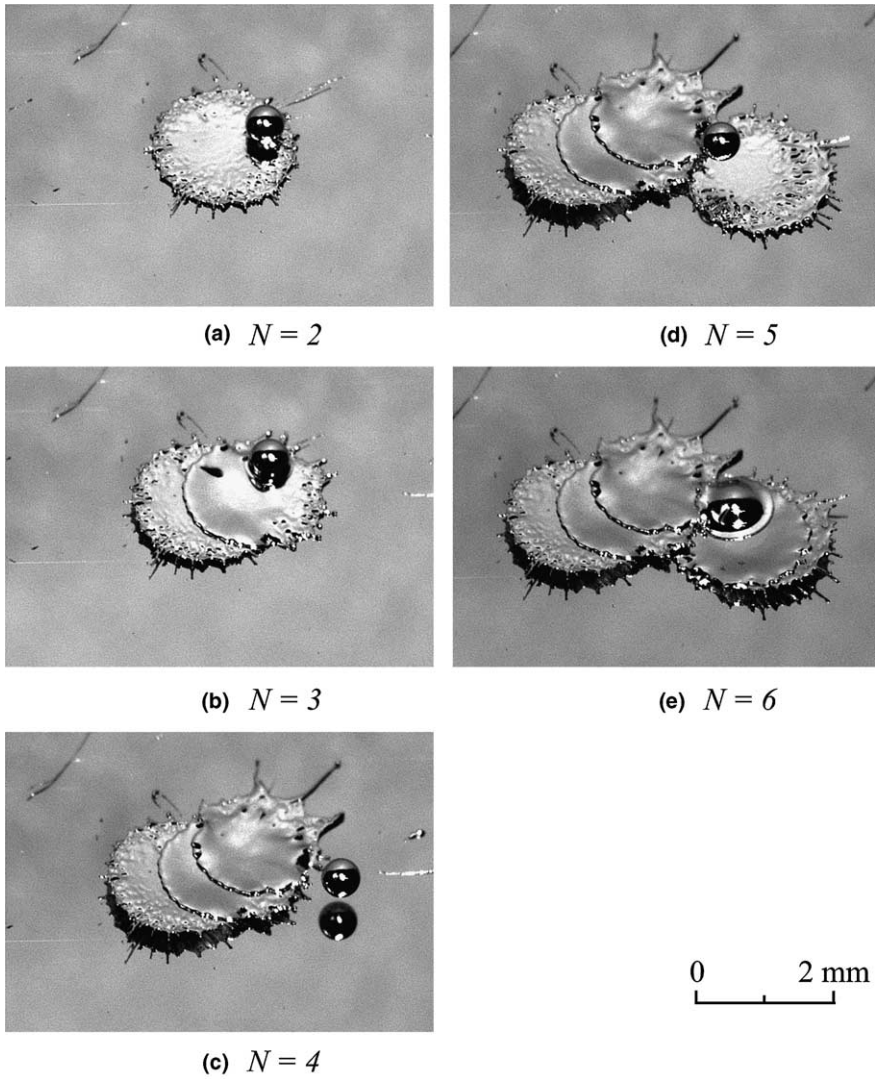

Fig. 5. Interactions of molten tin drops hitting a mirror-polished stainless steel surface at $T_{s,i} = 25$ °C. $V_0 = 10$ m/s, $Re = 21{,}818$, $We = 795$. N is the number of droplets in each photograph. The time interval between release of droplets is 2 s.

$$h^* = \frac{h}{D_0} = \frac{2\left(\frac{3}{8}We s^* + 3(1-\cos\theta_a) + \frac{4We}{\sqrt{Re}}\right)}{3(We+12)} \quad (6)$$

The dimensionless time taken by an impacting droplet to reach its maximum extension (t_c^*) has been estimated by Pasandideh-Fard et al. [19] as

$$t_c^* = \frac{8}{3} \quad (7)$$

Eq. (7) is valid, in principle, for all values of Re and We, and has been shown [10–12,19] to agree reasonably well with experimental measurements.

The criterion we use to determine the transition temperature is that it is the surface temperature for which the solid layer grows as thick as the splat in the time the droplet takes to spread to its maximum extent: in dimensionless form, $h^* = s^*$ at time $t^* = t_c^*$. Using $h^* = s^*$ in Eq. (6) gives the following expression for dimensionless solid layer thickness:

$$s^* = \frac{8\left[(1-\cos\theta) + \frac{4We}{3\sqrt{Re}}\right]}{3(We+16)} \quad (8)$$

Substituting Eqs. (7) and (8) in Eq. (3) we obtain the following expression for critical Stefan number (Ste_c, the Stefan number at which $T_{s,i} = T_t$):

$$Ste_c = \frac{APe}{2(We+16)}\left[(1-\cos\theta_a) + \frac{4We}{3\sqrt{Re}}\right]\frac{1}{\left[1 - \frac{\ln(1+BiA)}{BiA}\right]} \quad (9)$$

where

$$A = \sqrt{\frac{8\pi\gamma_d}{3Pe\gamma_s}} \quad (10)$$

The transition temperature (T_t) is given by

$$T_t = T_m - \frac{Ste_c H_{f,d}}{c_d} \quad (11)$$

3.3. Effect of contact resistance on transition temperature

Fig. 4 shows the calculated variation of transition temperature with impact velocity for 0.6 mm diameter tin droplets. Aziz and Chandra [10] measured the advancing contact angle (θ_a) of molten tin on a smooth polished stainless steel surface to be around 140°. Similar values of θ_a for tin on smooth aluminum and glass surfaces have been reported [20]. We used $\theta_a = 140°$ in all our calculations; a variation of ±20° in the magnitude of θ_a led to a variation of less than ±0.5% in the prediction of transition temperature. Since the contact resistance was unknown, curves are shown for three different values of R_c (10^{-6}, 10^{-7} and 0 m^2 K/W). The shaded region in Fig. 4 shows the observed range of transition temperature values. Assuming $R_c = 10^{-7}$ m^2 K/W gives predictions for the transition temperature in the range 155–160 °C, which agree reasonably with experimental observations (see Figs. 2 and 3).

Droplet impact velocity may either increase or decrease transition temperature, depending upon the value of the contact resistance; For $R_c < 10^{-7}$ m^2 K/W, T_t increases slightly with impact velocity, whereas for $R_c = 10^{-6}$ m^2 K/W, T_t decreases. Increasing impact velocity has two effects: it decreases both droplet spreading time and splat thickness. A smaller droplet spreading time implies that the solid layer has to grow faster to obstruct flow, so the transition temperature is lowered. However, as impact velocity increases, splat thickness diminishes and the solid layer has to grow to a smaller thickness, which increases transition temperature. The magnitude of contact resistance determines which of these two competing effects dominates. When R_c is low, the solid layer grows rapidly and spreading time variation is less important; for higher R_c, solid layer growth is slow and therefore transition temperature is determined by the time of droplet spreading. In either case the magnitude of the change is small, less than 10 °C, and difficult to detect in our experiments.

The effect of contact resistance on droplet splashing becomes evident during coating formation, when droplets land on previously solidified splats. Fig. 5 shows a sequence of photographs of six tin droplets landing sequentially with a velocity of 10 m/s, on a stainless steel substrate at 25 °C. The number of droplets deposited is indicated by N. In Fig. 5a the first droplet has spread out completely and solidified, with the splat showing evidence of splashing around its edges. The second droplet, released 2 s after the first, is just landing on the surface of the first splat. Once the second droplet spreads

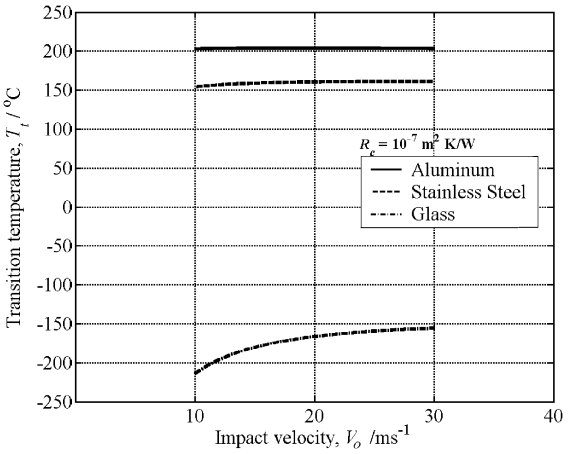

Fig. 6. Variation of transition temperature, T_t with impact velocity, V_0 for aluminum, glass and stainless steel surfaces. $R_c = 10^{-7}$ m^2 K/W.

(Fig. 5b) the portion of it in contact with the previous splat shows no sign of splashing while the part in contact with the steel substrate has splashed. The thermal contact resistance of the first splat, and of the air trapped under it, prevents solidification during spreading of the second drop, whereas the metal in direct contact with the substrate freezes rapidly and splashes. The same behavior is visible in impact of subsequent droplets (Fig. 5c–e), with long fingers forming along the periphery of the portion of the splat on the bare substrate, while the part on the previously deposited tin splats did not splash.

3.4. Effect of substrate material

The model for transition temperature predicts that it is a function of the substrate thermal property $\gamma_s = (\rho_s k_s c_s)$. Aluminum has a much higher value of γ_s (5.8×10^8 J^2 m^{-4} s^{-1} K^{-2}) than stainless steel ($\gamma_s = 5.8 \times 10^7$ J^2 m^{-4} s^{-1} K^{-2}), while γ_s for glass is much lower (1.5×10^6 J^2 m^{-4} s^{-1} K^{-2}). Calculated values of T_t are shown in Fig. 6 for all three materials. Assuming that $R_c = 10^{-7}$ m^2 K/W in all cases, the transition temperature on aluminum substrates is higher than that on stainless steel. The model predicts that we will never observe solidification induced splashing on a glass

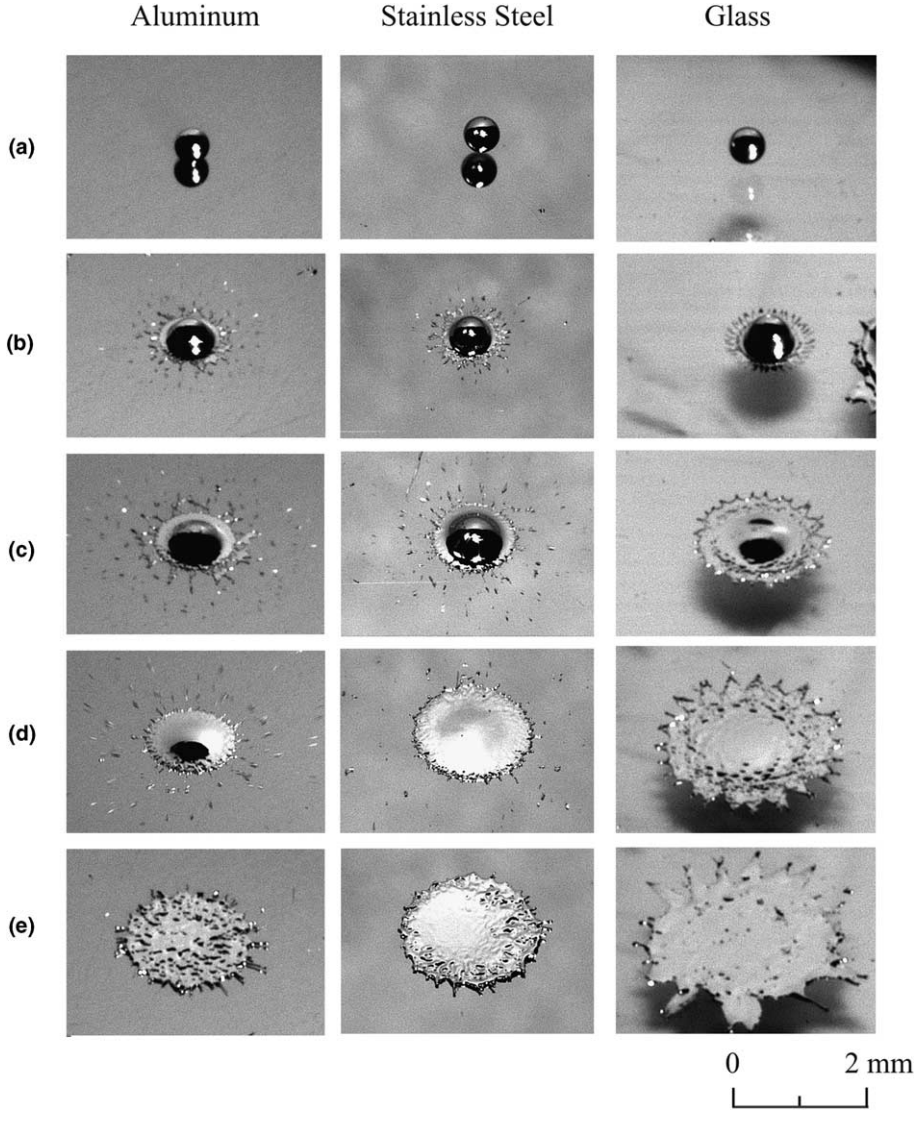

Fig. 7. Impact of molten tin drops with velocity 10 m/s on substrates of different materials at an initial temperature, $T_{s,i} = 25$ °C. The last picture in each column is the final solidified shape of the droplet. $Re = 21{,}818$, $We = 795$.

substrate maintained at room temperature, since the transition temperature is always far below that. Changing thermal contact resistance had little effect: setting $R_c = 0$ for glass raised T_t by only about 20 °C.

Photographs were taken of droplet impact on both aluminum and glass substrates. Fig. 7 shows three sequences of images showing the effect of substrate material on droplet impact dynamics. Substrate temperature was 25 °C and impact velocity was 10 m/s in all cases. The first column shows different stages of droplet impact on an aluminum substrate. The droplet splashed after impact and left a small splat that had a rough surface and edges. Splashing occurred on a stainless steel surface as well, but the final splat was a little larger and the centre of it was smooth, showing that solidification was slow enough for surface tension to smoothen the splat surface. There was no splashing on the glass surface, as predicted by the model. There were about 27 evenly spaced fingers around the periphery of the droplet (Fig. 7(d), glass substrate). A fluid dynamics model [17] of the instability around the edges of a spreading liquid droplet, without solidification predicts that the number of fingers is approximately:

$$N_f = 1.14We^{1/2} \tag{12}$$

Eq. (12) predicts 32 fingers, which agrees reasonable well with the number observed, supporting the hypothesis that they were created by fluid instabilities while the tin was still liquid.

Fig. 8 shows photographs of splats formed by impact of molten tin droplets on three different surfaces (aluminum, stainless steel and glass), at three different velocities (10, 20 and 30 m/s). All the droplets hitting the aluminum surface splashed, leaving small splats with rough surfaces. Droplets splashed on the stainless steel surface as well, but at the lowest velocity (10 m/s) the centre of the splat remained smooth. As impact velocity increased the size of this smooth area became smaller while the overall splat size increased. At high impact velocity splats become thinner and the solidification

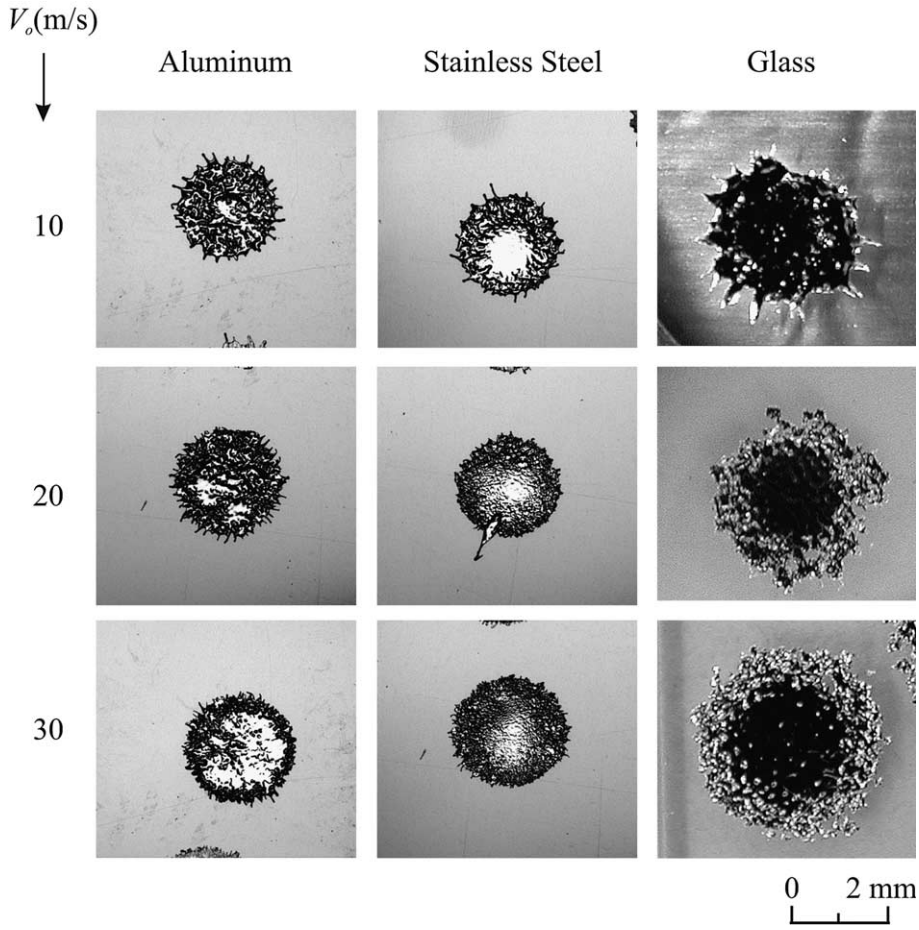

Fig. 8. Solidified splats of molten tin drops obtained on substrates of different materials held at an initial temperature, $T_{s,i} = 25$ °C with impact velocity, V_0.

front, which starts at the bottom and outer rim of the spreading droplet [13], reaches the centre before the surface can become even due to surface tension. On a glass surface there was no solidification induced splashing, even at the highest impact velocity. However, as velocity increased splat diameter became larger and there was more evidence of fluid instabilities along the edge of the spreading liquid droplet which produced irregular splats.

The transition to splashing on an aluminum surface can be seen in Fig. 9, which shows impact of droplets with 10 m/s velocity on substrates at 100 °C, 160 °C and 180 °C. At 100 °C break-up of droplets is clearly visible, at 160 °C the degree of break-up is diminished, while at 180° the droplet spreads into a disk-shaped splat without any splashing. The transition temperature in this case lies between 160 and 180 °C.

Fig. 10 shows the effect of varying impact velocity (10, 20 and 30 m/s) on splat shape at three surface temperatures (100 °C, 160 °C and 180 °C) on an aluminum substrate. At $T_{s,i} = 25°$ (see Fig. 8) and 100 °C the splats are small, having lost much of their original mass to splashing, and have a rough surface. At 160 °C the splats

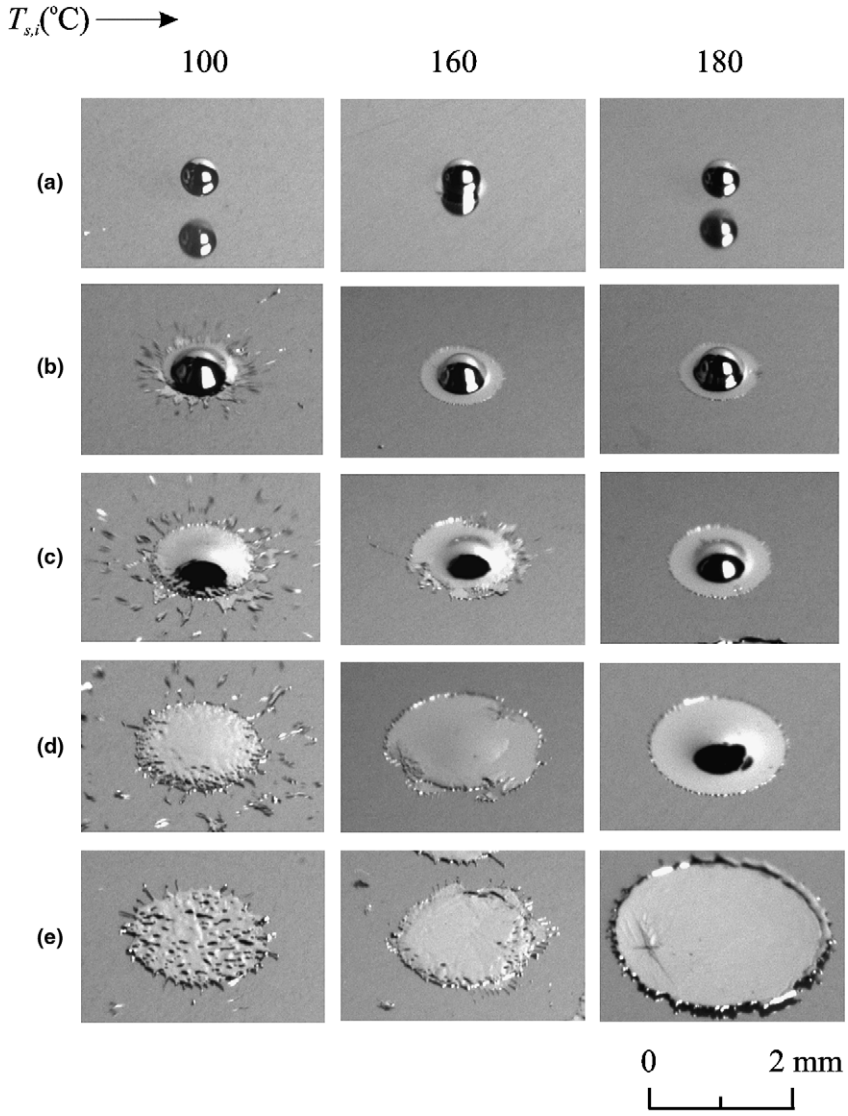

Fig. 9. Impact of molten tin drops with velocity 10 m/s on an aluminum surface at temperature: $T_{s,i}$ (i) 100 °C, (ii) 160 °C, (iii) 180 °C. The last picture in each column is the final solidified shape of the droplet. $Re = 21{,}818$, $We = 795$.

are larger, showing that the amount of splashing was reduced. There are several long fingers around the periphery of each splat, indicating that portions of the periphery remained liquid long enough for instabilities to develop and grow. At $T_{s,i} = 180$ °C and $V_0 = 10$ m/s the splat was almost perfectly round. At higher velocities ($V_0 = 20$ and 30 m/s) splat thickness was reduced and the presence of even the smallest protrusion on the surface was enough to obstruct liquid flow. Splats were therefore more irregular in shape.

The observed transition temperature on an aluminum surface was in the 160–180 °C range, lower than the value of 200 °C predicted by the model assuming $R_c = 10^{-7}$ m^2 K/W (see Fig. 6). Increasing the value of R_c decreased the predicted transition temperature. Fig. 11 shows predicted values of T_t for three different values of R_c. Observed values of T_t agree with predictions for R_c between 10^{-6} and 10^{-7} m^2 K/W. It is quite likely that contact resistance on an aluminum surface is greater than that on a steel surface: aluminum oxidizes rapidly and a surface oxide layer increases thermal resistance. Also, average roughness R_a for the aluminum substrate was 0.04 μm, higher than that for stainless steel and glass surfaces ($R_a = 0.01$ μm) since it was softer and more difficult to polish, which may also contribute to higher contact resistance.

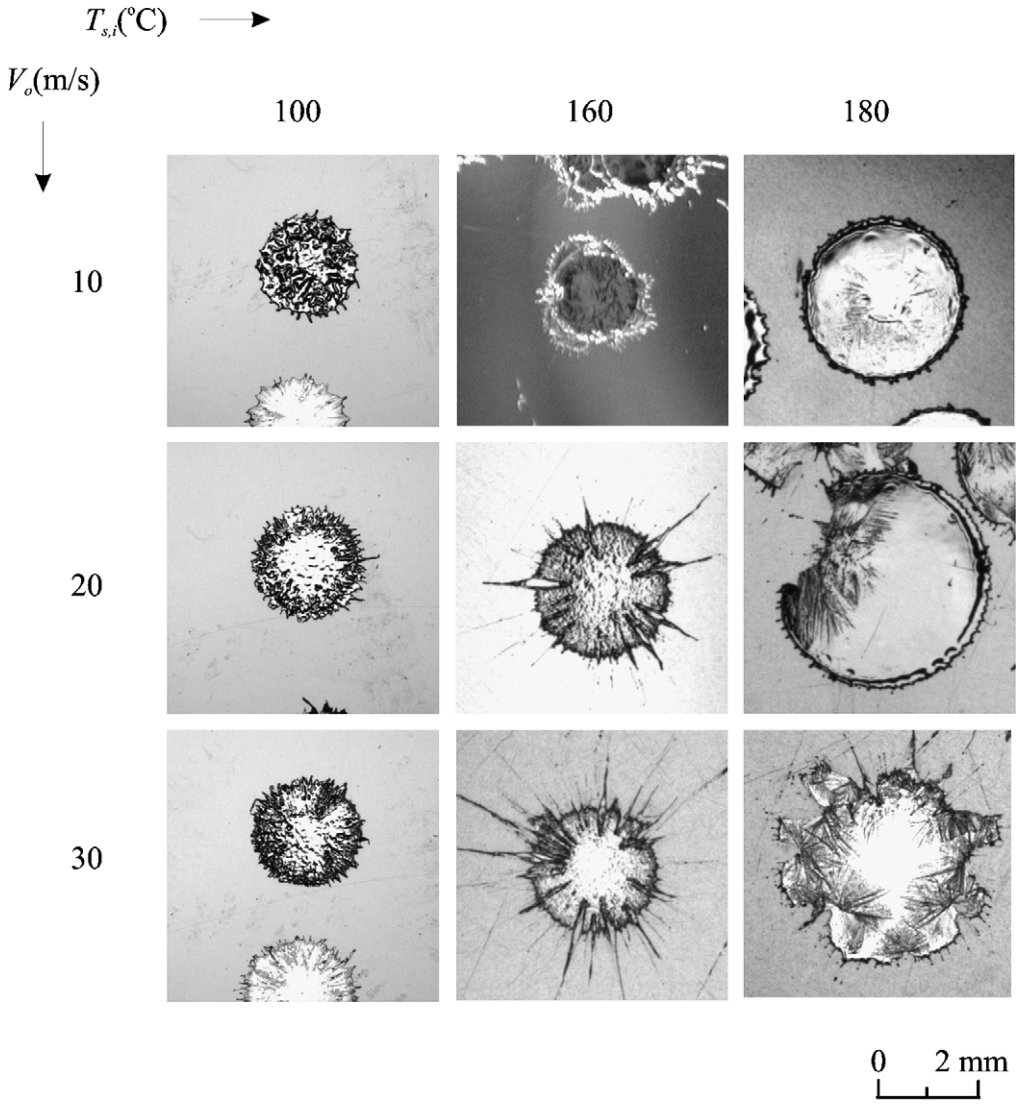

Fig. 10. Solidified splats of molten tin drops obtained on aluminum surfaces with impact velocity, V_0 and substrate temperature, $T_{s,i}$.

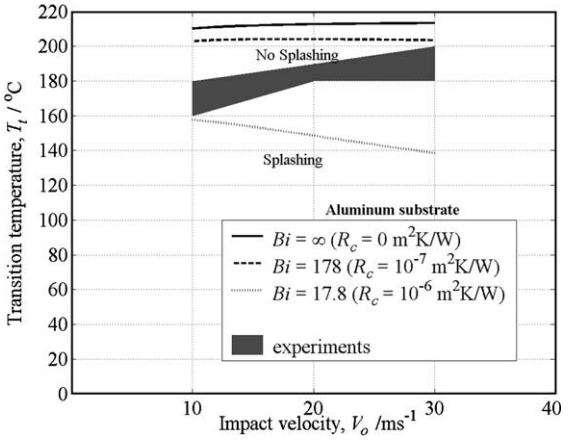

Fig. 11. Variation of transition temperature, T_t for aluminum substrate with impact velocity, V_0 for different values of contact resistance, R_c at the droplet–substrate interface.

4. Conclusions

Molten tin droplets impacting a surface with velocities varying from 10 to 30 m/s splash after impact on a cold surface, losing a significant portion of their mass in small fragments that detach from the periphery of the splat. On a hot surface there was no splashing and droplets spread to form disk-like splats with smooth edges. Solidification around the edges of spreading droplets created a solid rim that obstructed flow and triggered splashing. An analytical model was developed to predict the transition temperature at which splashing disappeared by assuming that the thickness of the solid layer had to equal that of the splat in the time the droplet spread to its maximum extent in order to obstruct liquid flow. The model predicted the transition temperature for aluminum and stainless steel surfaces if we assumed that $R_c = 10^{-6}$–10^{-7} m^2 K/W. The model also predicted that tin droplets would not splash on glass surfaces maintained at or above room temperature, and this was confirmed by experiments.

Acknowledgements

The authors would like to acknowledge financial support for this research from the Natural Sciences and Engineering Research Council of Canada (NSERC) and Materials and Manufacturing Ontario (MMO).

References

[1] L. Bianchi, A.C. Leger, M. Vardelle, A. Vardelle, P. Fauchais, Splat formation and cooling of plasma-sprayed zirconia, Thin Solid Films 305 (1997) 35–47.

[2] C.J. Li, J.L. Li, W.B. Wang, A. Ohmori, Effect of particle substrate materials combinations on morphology of plasma sprayed splats, in: C. Coddet (Ed.), Proceedings of the 15th International Thermal Spray Conference, ASM International, Materials Park, OH, 1998, pp. 481–487.

[3] H. Zhang, X.Y. Wang, L.L. Zheng, X.Y. Jiang, Studies of splat morphology and rapid solidification during thermal spraying, Int. J. Heat Mass Transfer 44 (2001) 4579–4592.

[4] C.J. Li, J.L. Li, W.B. Wang, The effect of substrate preheating and surface organic covering on splat formation, in: C. Coddet (Ed.), Proceedings of the 15th International Thermal Spray Conference, ASM International, Materials Park, OH, 1998, pp. 473–480.

[5] X. Jiang, Y. Wan, H. Hermann, S. Sampath, Role of condensates and adsorbates on substrate surface on fragmentation of impinging molten droplets during thermal spray, Thin Solid Films 385 (2001) 132–141.

[6] J. Pech, B. Hannoyer, A. Denoirjean, P. Fauchais, Influence of substrate preheating monitoring on alumina splat formation in DC plasma process, in: C.C. Berndt (Ed.), Proceedings of the 1st International Thermal Spray Conference, ASM International, Materials Park, OH, 2000, pp. 759–765.

[7] M. Fukomoto, Y. Huang, Flattening mechanism in thermal sprayed Ni particles impinging on flat substrate surface, J. Thermal Spray Technol. 8 (3) (1999) 427–432.

[8] C.J. Li, H.L. Liao, P. Gougeon, G. Montavon, C. Coddet, Effect of Reynolds number of molten spray particles on splat formation in plasma processing, in: B. Marple, C. Moreau (Eds.), International Thermal Spray Conference, ASM International, Materials Park, OH, 2003, pp. 875–882.

[9] Y.P. Wan, H. Zhang, X.Y. Jiang, S. Sampath, V. Prasad, Role of solidification, substrate temperature and Reynolds number on droplet spreading in thermal spray deposition: measurements and modelling, ASME J. Heat Transfer 123 (2004) 382–389.

[10] S.D. Aziz, S. Chandra, Impact, recoil and splashing of molten metal droplets, Int. J. Heat Mass Transfer 43 (2000) 2841–2857.

[11] M. Pasandideh-Fard, R. Bhola, S. Chandra, J. Mostaghimi, Deposition of tin droplets on a steel plate: simulations and experiments, Int. J. Heat Mass Transfer 41 (1998) 2929–2945.

[12] S. Shakeri, S. Chandra, Splashing of molten tin droplets on a rough steel surface, Int. J. Heat Mass Transfer 45 (2002) 4561–4575.

[13] N.Z. Mehdizadeh, M. Raessi, S. Chandra, J. Mostaghimi, Effect of substrate temperature on splashing of molten tin droplets, ASME J. Heat Transfer 126 (3) (2004) 445–452.

[14] CHR. Mundo, M. Sommerfeld, C. Tropea, Droplet–wall collisions: experimental studies of the deformation and breakup process, Int. J. Multiphase Flows 21 (2) (1995) 151–173.

[15] S.X. Cheng, T. Li, S. Chandra, Producing molten metal droplets with a droplet-on-demand generator, J. Mater. Sci. Technol. 159 (2005) 295–302.

[16] R. Dhiman, Coating formation by sequential impact of molten tin droplets, M.A.Sc. Thesis, University of Toronto, Toronto, ON, Canada, 2003.

[17] N.Z. Mehdizadeh, S. Chandra, J. Mostaghimi, Formation of fingers around the edges of a drop hitting a metal plate with high velocity, J. Fluid Mech. 510 (2004) 353–373.
[18] D.R. Poirier, E.J. Poirier, Heat Transfer Fundamentals for Metal Casting, second ed., Minerals, Metals and Materials Society, Warrendale, PA, 1994, pp. 41–42.
[19] M. Pasandideh-Fard, Y.M. Qiao, S. Chandra, J. Mostaghimi, Capillary effects during droplet impact on a solid surface, Phys. Fluids 8 (3) (1996) 650–659.
[20] N. Eustathopoulos, M.G. Nicholas, B. Drevet, Wettability at High Temperatures, first ed.Pergamon Materials Series, vol. 3, Oxford, UK, 1999, pp. 202, 240, 137–138.